Journal of Fluids and Structures (1999) **13,** 61–73
Article No.: jfls. 1998.0191
All articles available online at http://www.idealibrary.com.on IDEAL

EXPERIMENTAL FLOW STUDY WITHIN A SELF OSCILLATING COLLAPSIBLE TUBE

K. KOUNANIS AND D. S. MATHIOULAKIS

Department of Mechanical Engineering, National Technical University of Athens Heröon Polytechniou 9, Zografos 15773, Athens, Greece

(Received 26 September 1997 and in revised form 12 June 1998)

The flow field within a self-excited flexible tube was studied by employing flow visualization, velocity and pressure measurements. Under low positive tansmural pressures at the tube inlet (of the order of 50 mm H_2O) the tube was set to an oscillatory motion, the initiation of which was due to a flow asymmetry. Namely, although initially the flow was separated from both sides of the formed divergent nozzle close to the tube outlet, at an arbitrary instant this became attached to one side, but stayed separated in the remaining part of the nozzle. When this flow asymmetry occurred, the walls approached each other and the tube neck formed there by started oscillating streamwise, setting the tube to an oscillatory motion. During the downstream motion of the tube neck, it was shrunk, causing a twofold increase of the local velocities compared to the inlet ones, which remained almost constant. On the contrary, when moving upstream, the tube neck expanded, causing a flow reversal in this area and a flow deceleration in the remaining part of the tube. The pressure signals upstream and downstream of the tube exhibited a phase difference, the latter leading, taking an order of magnitude higher values than the first one.

1. INTRODUCTION

THE FLOW BEHAVIOUR within a flexible tube and its wall motion has been the object of research in the past years, mainly due to many physiologic applications (flow in arteries–veins, lung airways, urethra, etc.), but also due to interesting flow phenomena which take place, such as unsteady flow separation, vortex shedding and flow choking.

The basic feature which makes the prediction of the fluid–solid interaction difficult in this particular problem is that due to low bending tube stiffness under low transmural pressure values, pressure perturbations of small amplitude result in significant deformations of the tube cross-sectional area. This area change implies variation of the fluid momentum as well as of the pressure distribution along the tube axis, which again affects the shape of the tube. This succession of momentum–pressure–shape changes culminate in self-excitation of the flexible tube which, under certain conditions, is involved in periodic or nonperiodic (chaotic) oscillations.

In the existing literature, tube materials that have been tested most are the so-called Penrosetubing, used as surgical drainage tubing, and silicone rubber, due to their resemblance to the elastic properties of the human veins and arteries. These properties are described normally by a "tube law", namely a nonlinear relationship of the transmural pressure versus tube area. In the experiments, the well-known "Starling resistor" configuration is normally used, where the elastic tube is enclosed in an airtight chamber of

0889–9746/99/010061 + 13 $30.00

controllable pressure, whereas the tube internal pressure is adjusted by employing two constrictions, one upstream and the other downstream of the tube, of variable resistance.

Based on a Starling resistor, Conrad (1969) first presented systematic experimental pressure flow curves for both steady and unsteady flow inlet conditions of a Penrose tube, proposing also an electric analog to provide explanations for its oscillatory motion in the negative slope section of the pressure-drop versus flow-rate curve. Conrad's experimental data were interpreted by Griffiths (1971), borrowing ideas from the one-dimensional compressible flow theory, considering that the fluid in the collapsible state of the tube goes from a subsonic to a supersonic state, where sonic is the case that the fluid speed is equal to the phase speed. In later work, Conrad *et al.* (1978) demonstrated an aspect of the complex phenomenon of the tube self-oscillations by using a cavity of variable length downstream of the flexible tube, according to which the frequency of oscillations was very much dependent on this length. Elliot & Dawson (1978) examined both analytically and experimentally a stable supercritical (supersonic) flow in a Penrose tube, where speed ratios (fluid to sonic) up to 10 were measured. The longitudinal tension of the tube as well as fluid wall friction affected the pressure variation along the elastic jump which appeared in their experimental set-up. They also showed how a combination of the continuity and momentum equations end up in a hyperbolic equation for the perturbation of the tube area, so that when the flow is supercritical there are only downstream traveling disturbances. Kamm & Shapiro (1979), in an extended work, examined the flow within a flexible tube both experimentally and analytically by employing a one-dimensional linear and nonlinear theory for the solution of the continuity and momentum equations combined with a tube law. Brower & Sholten (1975) measured the phase speed c as a function of the transmural pressure, P, where

$$c = \sqrt{\frac{A}{\rho}\frac{dP}{dA}},$$

in which A is the tube area, and ρ the fluid density. They showed that the fluid velocity u, when the tube is in a state of collapse can be equal or greater than c, a condition responsible for flow instabilities. This inequality is explained by the fact that under this condition the tube area becomes very small and therefore u becomes large, whereas due to small values of $\mathrm{d}P/\mathrm{d}A$, c takes small values. Morgan & Parker (1989) used a one-dimensional flow model, solved numerically, to compare their pressure-drop versus flow-rate curves with existing experimental ones.

Barclay & Thalayasingan (1986) measured the frequency of oscillations for various Reynolds numbers and tube lengths. They realized that for the silicone rubber tube they used, oscillations started at Re higher than 1500, which is higher than the Re of the blood flow in veins and arteries. Bertram (1986) examined experimentally the self-oscillations of a flexible tube with thick walls by varying the downstream constriction and the pressure chamber of a Starling resistor. He found a wide band of frequencies of periodic or chaotic nature, with the upstream pressure and flow amplitudes being much smaller than their downstream counterparts. Cancelli & Pedley (1985) developed a one-dimensional model including an energy loss term, allowing streamwise oscillation of the separation point, based on pressure gradient values. This motion was according to the authors the primary reason for the tube oscillations.

The significance of axial tension with regard to the onset of tube oscillations was examined by Pedley (1992) in a mathematical study. It was shown that, due to the fluid wall-shear, this tension takes on smaller and smaller values in the streamwise direction so that eventually the wall membrane, becoming unstretched, is easier to flutter. The instabilities of the tube oscillations were examined by Jensen (1992), employing a one-dimensional

model, with a modified tube law in which longitudinal stresses were taken into account, while energy losses were included in a term in the momentum equation.

Elad *et al.* (1992) measured the three-dimensional structure of a collapsible tube via photography under steady flow conditions, and their extracted tube laws compared well with published ones. Matsuzaki *et al.* (1994) introduced a model for the case of a collapsible channel, in which the wall stiffness was taken into account by considering it to be supported by a series of springs. They examined how the channel shape and pressure distribution were affected, by considering the flow to be separated or attached, as well as the effect of several parameters upon the pressure drop through the channel, such as external pressure, wall thickness, downstream pressure and downstream rigid tube length.

Ribreau *et al.* (1993) studied numerically the collapse of a flexible tube, calculating the transmural pressure as a function of wall thickness and ellipticity (major to minor axis ratio of the elliptical cross section) under which two opposite points of the tube perimeter first touch each other, and then, by gradually lowering the pressure, more points come into contact along a stright line, for the most frequently occurring case of bimodal collapse. However, it was shown by Dion *et al.* (1995) both theoretically and experimentally that in the most general case, a collapsible membrance under a uniform pressure can be deformed to a shape with n symmetry axes, where $n \geq 2$, and that the higher the number n is, the lower the transmural pressure has to be.

Bertram *et al.* (1994) and Bertram & Godbole (1995) measured the tube area distribution as a function of time along a self-oscillating tube of constant frequency, using the exit pressure as a triggering mechanism for phase averaging.

In the present work, the flow field within a self-oscillating transparent flexible tube was studied experimentally by employing flow visualization, velocity and pressure measurements.

2. EXPERIMENTAL SET-UP

The experimental work presented in this paper was conducted in two laboratories, namely in the Laboratory of Hydraulic Machines of the National Technical University of Athens (NTUA) and in the Biomedical Engineering Laboratory of the Swiss Federal Institute of Technology at Lausanne (EPFL). The experimental rig in both laboratories included a Stalring resistor, namely water flowed by gravity between two water tanks at a certain difference in elevation through a flexible tube; the external pressure, P_e, was maintained constant. In order to eliminate gravity effects and facilitate velocity measurements by Laser Doppler Velocimetry (LDV), the flexible tube was surrounded by stationary water. In NTUA an airtight chamber made of plexiglas was used, where P_e was adjustable through a manual air pump. The volume of this chamber was 1000 times greater than the flexible tube volume, so that any deformations of the tube did not affect P_e. In EPFL, this chamber was open at the top, necessary for the LDV probe to approach the tube, due to its small focal length (45 mm). Additionally, one adjustable constriction, R_1, was located upstream of the tube and another one, R_2, downstream of it, so that both pressure and flow rate could be varied. The geometric details of the two experimental rigs are included in Table 1, where l_1, l_2 are the lengths of the rigid tubes upstream and downstream of the flexible one, and h_1, h_2 are the elevation of the latter with respect to the upper and lower tank, respectively.

Concerning the flexible tube, its material was a silicon elastomer made at EPFL (see Pythoud *et al.* 1994) with an internal diameter of 8 mm and wall thickness 0·2 mm, having the advantage of being transparent, thus allowing both LDV measurements and flow visualization. The length of the tube was 80 mm, connected to rigid tubes of 7 mm internal diameter, being unstretched both in the radial and longitudinal direction.

TABLE 1

Geometric characteristics of hydraulic installations at NTUA and EPFL

	NTUA (mm)	EPFL (mm)
l_1	5000	2000
l_2	8000	1500
h_1	− 1700	− 1150
h_2	220	650/350/150

Flow visualization in the interior of the tube was performed using white particles of almost neutral buoyancy, an He–Ne laser sheet (power 10 mW) oriented vertically along the tube axis and normal to the plane of collapse, and a CCD video camera. These pictures were stored by a VCR (SONY-SVO 5800P) in a video tape along with a time code which allowed the selection of a particular picture and its digitization by a frame grabber (Targa plus).

The parameters which were recorded during the experiments were pressure, axial velocity, and flow rate.

In NTUA gauge pressures within the flexible tube were measured using pressure catheters (Millar 5P) while strain gauge pressure transducers (KYOWA-611) were employed to measure the external pressure P_e as well as the pressure drop through the flexible tube. The streamwise velocity component was measured by a one component LDV (with an He–Ne laser of 17 mW as a light source) operating in the forward scattering mode, including a Bragg cell for negative flow detection, a frequency shifter (DISA 55N10) and a counter (DISA 55L90) as a signal processor. The flow rate was measured with an electromagnetic flowmeter (Fischer–Porter) installed upstream of the flexible tube. The analog outputs of the pressure, speed and flow rate measuring systems were digitized by an A/D converter (PCL818 of Advantech) with a sampling frequency of 400 Hz per channel (maximum throughput 100 kHz).

In EPFL, pressure was measured by pressure catheters (Millar 2F). The fluid velocity was measured by using one of the three components of a LDV system, operating in back scattering mode. The light source was an argon ion laser (5 W), and the signal processor a burst spectrum analyzer (BSA, type 57N10) made by DANTEC. The output signal was fed to a personal computer through a National Instruments PC2-A board. The traversing system was 3-D and fully automated, made by DANTEC (type 57G15), facilitating the movement of the LDV probe to a prescribed number of measuring points. Finally, the flow rate was measured by a transit time ultrasound flowmeter (TRITON) installed in the flexible tube (since this type of flowmeter could not operate when the fluid is surrounded by solid walls). The pressure and flow rate signals were digitized by an A/D with a frequency of 500 Hz.

3. RESULTS AND DISCUSSION

In the context of this work, emphasis was given upon the investigation of the self-excited oscillations of a flexible tube. In order to detect this kind of oscillation the transmural pressure (defined as the internal minus the external pressure at the tube inlet) had to take low positive values, for the tube to become compliant and consequently easier to oscillate. To make this happen, the procedure followed was to increase progressively the upstream resistance R_1, resulting in a reduction of both the flow rate and the pressure inside the tube,

while keeping the downstream resistance R_2 constant. Therefore, starting from a distended state, the tube was set to self-induced oscillations when the transmural pressure became low enough (of the order of 50 mm H_2O). Before the onset of oscillations, the tube took the shape of a convergent–divergent nozzle, whose neck was located about two diameters upstream of its exit. The location of this neck is the result of balance of various forces exerted upon the membrane of the tube as well as its material properties, such as the forces due to the transmural pressure, fluid wall-shear stress, tube axial tension, axial, and circumferential tube wall bending stiffness (Pedley 1992).

Once the divergent nozzle was formed, it was observed through flow visualization that flow separation took place a little downstream of the tube neck, so that essentially there was a jet at the tube axis surrounded by stagnant fluid, whose width varied with time, normally in a chaotic way. When the flow field was symmetric about the jet axis (Figure 1), there were some motions of the tube wall of small amplitude, predominantly normal to the plane of collapse which was horizontal. However, at an arbitrary instant, without changing externally the flow conditions, the flow became attached at the upper wall of the nozzle (it should be recalled that the light sheet was vertical, lighting only two sides of the nozzle) and separated in the remaining part of the cross-section (Figure 2). When this asymmetry occurred, oscillations started. Specifically, initially the opposite sides of the nozzle approached each other, reducing the neck area, which then moved to the downstream end of the tube, opened and repeated the same cycle. More particularly, at a distance of about one diameter upstream of the tube exit, the opposite sides of the neck came into contact, forcing the fluid to take high speeds there, thus reducing the static pressure at this point as well as downstream of it, due to essentially no pressure recovery in the separated flow region of the formed divergent nozzle. This pressure reduction resulted in a further collapse of the tube in the streamwise direction, till the neck approached the downstream end of the tube. At the same time, the kinetic energy of the upstream fluid due to the closing process of the tube was converted to a pressure increase which, combined with the tube stresses acted in the opposite direction, tending to bring the tube to its initial distended state. During these oscillations the flow field was quite symmetric.

The foregoing are depicted clearly in a sequence of 10 pictures (Figure 3) for $P_e = 200$ mm H_2O and a mean flow rate of $\bar{Q} = 1340$ ml/min, showing the deformation of the tube outlet section from an open state to a completely collapsed one, and back to open. In each picture a time code is included, an increment of which by one digit corresponds to a time interval of 40 ms. Basic conclusions drawn from these picture are as follows.

(a) During the phase of collapse the tube cross-section resembled the infinity symbol (∞), as seen in pictures 4 to 7, with the opposite walls being closer on the plane of illumination. Since the camera axis was horizontal and parallel to the plane of collapse, the tube longitudinal cross-section was recorded as having two bright and two faint boundaries, where the first, being closer to each other, corresponded to the illuminated plane at the tube centre.

(b) The particle paths designed the separated flow region of the divergent nozzle (crossing trajectories) as well as the jet limits (parallel trajectories).

(c) The time interval for the formation of the tube neck and its complete collapse lasted more than 10 times (pictures 1–8; or 600 ms) than its reopening (picture 9, less than 40 ms). The same trend, although not with the same time ratios, was observed under all the conditions of P_e examined and constriction settings of R_1 and R_2. The characteristic collapse of the tube at its downstream edge is shown in more detail in Figure 4.

Besides flow visualization, static pressures were recorded 140 mm upstream (P_u) and downstream (P_d) of the oscillating tube via two pressure catheters. In order to obtain pictures in phase with the pressure signals, the following procedure was followed: the output

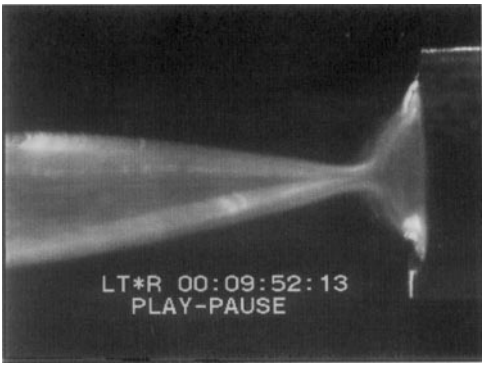

Figure 4. The tube neck at the tube exit.

of a video camera was stored in a video tape, along with the time code of the pictures. At the arbitrary instant that pressure measurements were initiated, a trigger pulse was sent to the camera, the output of which (one picture with its time code) was digitized, while at the same time pictures were still being recorded in the video tape. Thus, knowing the time code of this particular pictures that the pressure measurements started, all pictures recorded later, were in phase with the pressure signals.

Time records of P_u and P_d are included in Figure 5, with the symbols corresponding to the pictures of Figure 3. It is interesting to notice a phase difference between the pressure signals P_u and P_d, the latter leading. That is, the downstream pressure starts being reduced first (picture 4 of Figure 3), whereas the upstream pressure starts increasing 120 ms later (picture 7 of Figure 3), namely a little before the necking approaches the outlet of the tube. After the tube is closed, the pressure increases upstream of it but not significantly (compared to the reduction of P_d), due to the flexibility of the duct which acts as a pressure damper. In contrast, due to the rigid walls of the downstream tube, P_d takes low values (not shown in Figure 5) during the fluid deceleration when the tube collapses, which in this particular case was 3100 mm H_2O (as a minimum) below atmospheric. Another feature observed in the same figure is that both signals exhibit peaks and valleys, besides those which correspond to the closing and opening of the duct, due to the reflected pressure waves associated with this process.

The pressure distribution along the tube axis, x ($x = 0$ coincides with its outlet and $x > 0$ points streamwise) was obtained by traversing a pressure catheter. Figures 6 and 7 include the time-mean pressure distribution and its standard deviation, respectively, for $P_e = 200$ mm H_2O, $\bar{Q} = 1400$ ml/min, and $P_e = 400$ mm H_2O, $\bar{Q} = 1300$ ml/min. At the tube outlet ($x = 0$) there is a stepwise pressure reduction and a small recovery, whereas pressure fluctuations, being strong in the same area, are attenuated in the downstream direction. This high pressure drop through the tube is attributed to the fact that the pressure upstream of the tube neck takes values close to P_e (since the transmural pressure has to be close to zero for the tube to be compliant under this state of oscillation), whereas P_d is independent of P_e, taking mean values which correspond to the flow losses from this point to the low-level water tank of the hydraulic installation; i.e. $\bar{P}_d$ is related monotonically to the flow rate. In order to minimize the influence of the catheter upon the flow field, it was not positioned in the region where the tube neck was oscillating; otherwise, it was observed that the frequency of oscillation was changed (sometimes the tube even stopped oscillating) and the flow rate was reduced.

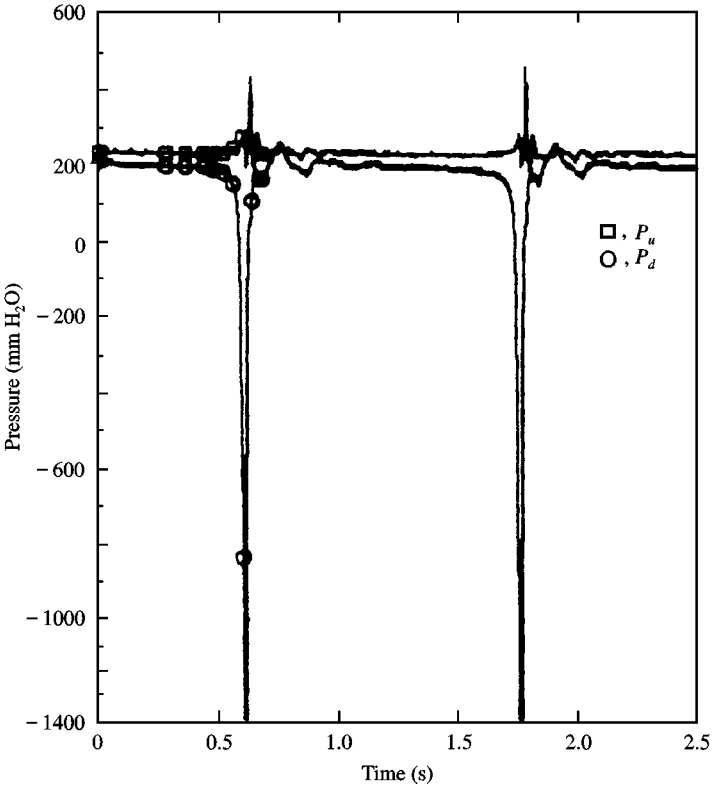

Figure 5. Pressure signals in phase with the pictures of Figure 3.

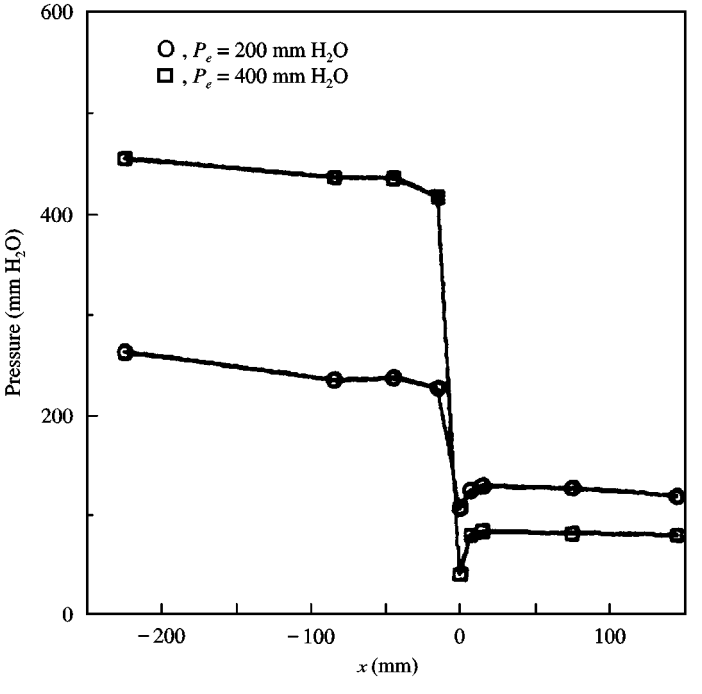

Figure 6. Time-mean pressure distribution along the tube.

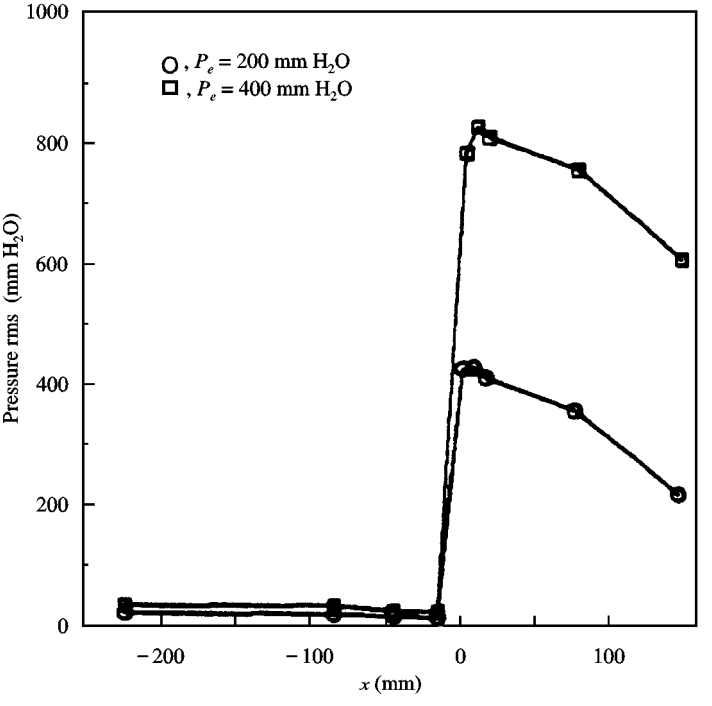

Figure 7. Pressure fluctuations (r.m.s.) along the tube.

Simultaneous measurements of P_u and P_d 140 mm upstream and downstream of the tube, as well as the streamwise velocity component at the centre of the duct at various locations x, were also taken at NTUA when the transparent tube was oscillating, for $P_e = 200$ mm H_2O and $\bar{Q} = 1100$ ml/min. The most striking feature of the velocity temporal variation along the tube is that although upstream of the duct its fluctuations are mild, close to its exit and downstream of it these are very strong. More particularly, the velocity varies upstream of the duct ($x = -100$ mm) between 50 and 60 cm/s [Figure 8(a)], whereas close to its exit [$x = -4$ mm, Figure 8(b)] and downstream of it [$x = 40$ mm, Figure 8(c)] this takes values from negative to almost twice that at its inlet. In Figure 8, when P_d drops, which means that the tube starts collapsing, the fluid accelerates with a high rate due to both the reduction of the tube cross-section and the shrinkage of the tube volume. On the contrary, when the tube expands there is a fluid deceleration, leading to even negative values at the centre of the tube close to its exit ($x = -4$ mm). Due to low values of P_d, this has been truncated in Figure 8 (as in Figure 5), so that the temporal variations of the three signals are shown better.

Detailed velocity measurements were also performed at EPFL using a BSA as signal processor, which proved to respond more reliably than the counter (use in NTUA) to the fast changes of the flow field. At $x = -3$ mm (Figure 9) the fluid velocity time record was similar to the one examined at NTUA, taking however higher negative values (-125 cm/s), for a mean flow rate of 800 ml/min (mean velocity 26·53 cm/s), $P_e = 30$ mm H_2O and $h_2 = 650$ mm. When the velocity changed sign from positive to negative and for a period of about 50 ms, the LDV system did not accept valuable data, apparently due to the complete collapse of the tube which did not allow the crossing of the Laser beams (for instance from point A to point B of Figure 9). Upstream of $x = -14$ mm, the velocity did not take any

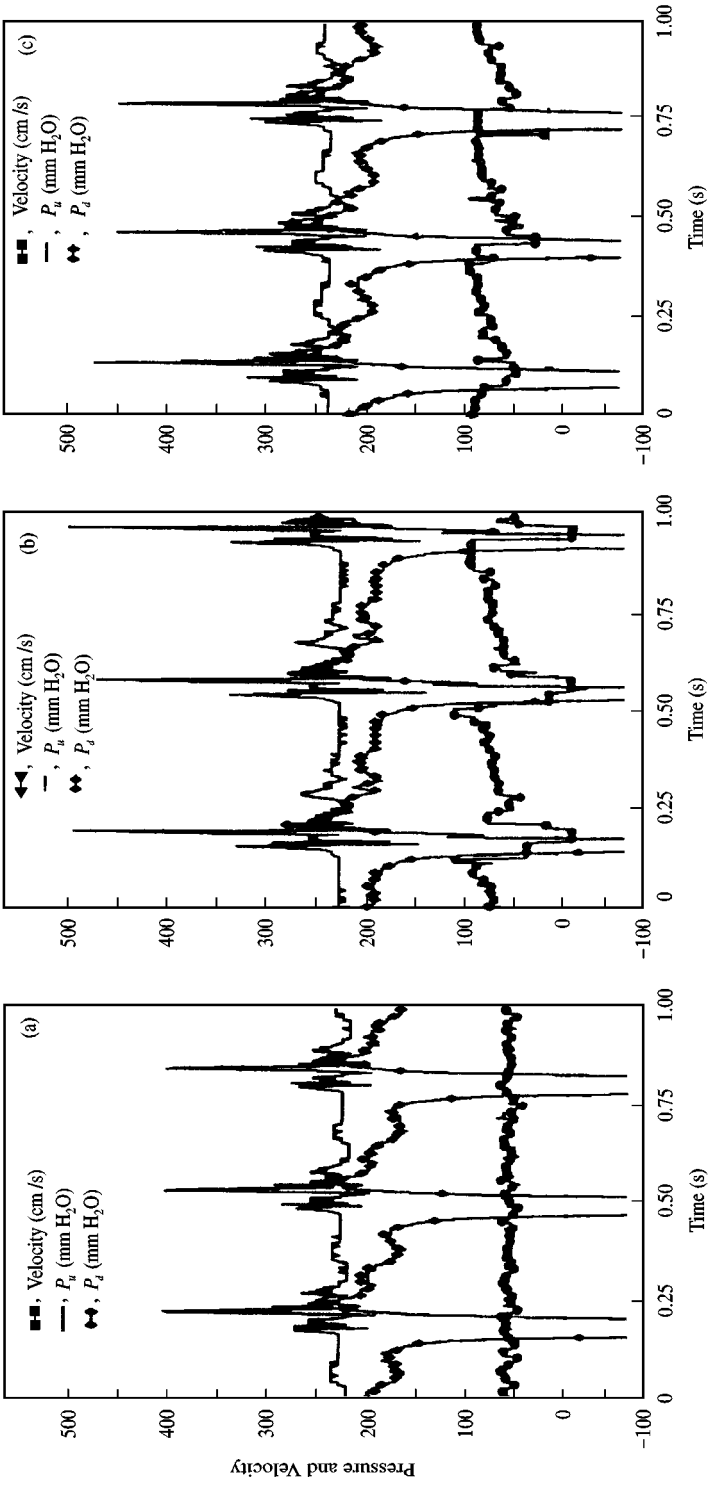

Figure 8. Time records of pressure and velocity: (a) $x = -100$ mm; (b) $x = -4$ mm; (c) $x = 40$ mm.

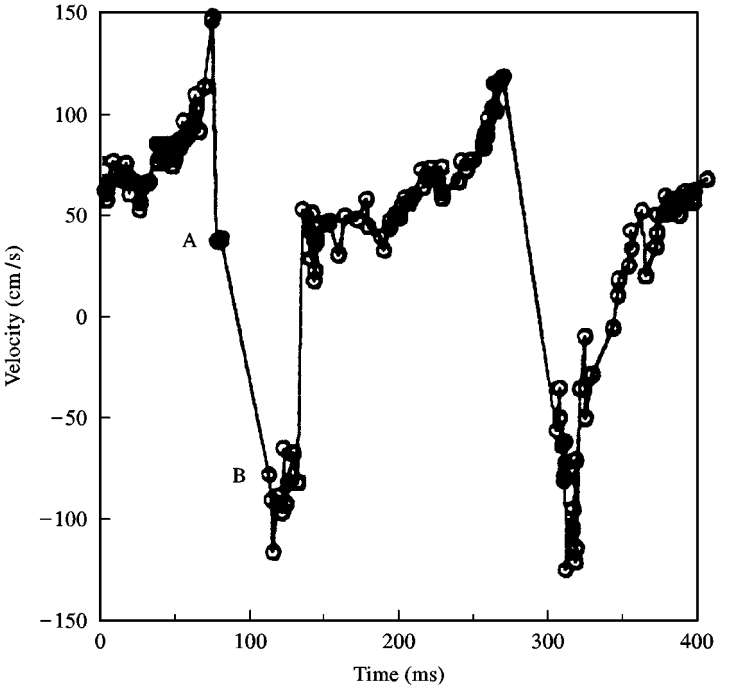

Figure 9. Time record of velocity ($x = -3$ mm).

negative values, which means that the axial motion of the tube neck is from this point toward the tube exit (also verified by flow visualization) since an abrupt increase of the tube volume in this region (during the tube opening) causes a flow reversal. Moving further upstream, there is an attenuation of the velocity amplitude (e.g. $x = -20$ mm, Figure 10), while upstream of $x = -30$ mm the characteristic frequency of oscillations is obscured by other frequencies. This amplitude attenuation is attributed to the small time derivative of the tube volume, since towards its inlet the tube wall displacements become progressively small. Downstream of the flexible tube, the velocity increases almost linearly with time ($x = 55$ mm, Figure 11) from zero to a peak value of 150 cm/s and then back to zero almost instantly. This variation can be explained by the continuity equation,

$$Q_{\text{in}} - Q_{\text{out}} = \frac{\partial V}{\partial t}, \tag{1}$$

where Q_{in} and Q_{out} are the inlet and outlet flow rates, and V the volume of the tube. Therefore, when the tube shrinks, or $\partial V/\partial t < 0$, then $Q_{\text{in}} < Q_{\text{out}}$. The opposite happens when the tube expands. Since Q_{in} is almost constant, when the flow accelerates in this region, both tube expansion (first) and shrinking (next) take place.

Finally, the frequency of flow oscillations was examined for several cases. It was observed that for all combinations of P_e, R_1 and R_2 settings, there was a trend for this frequency to be increased with increasing values of $P_e - \bar{P}_d$ [the same tendency was also observed by Bertram (1986)], without however being able to find a definite relationship between these

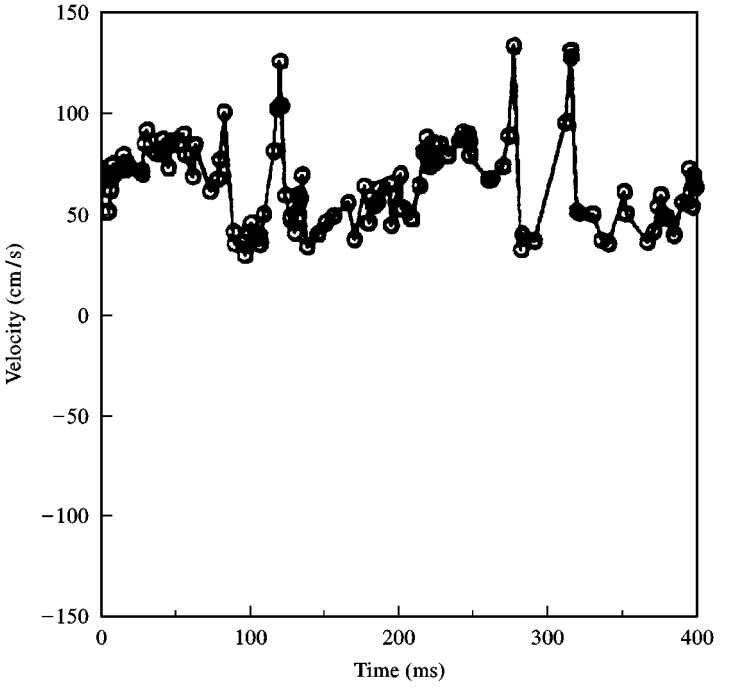

Figure 10. Time record of velocity ($x = -20$ mm).

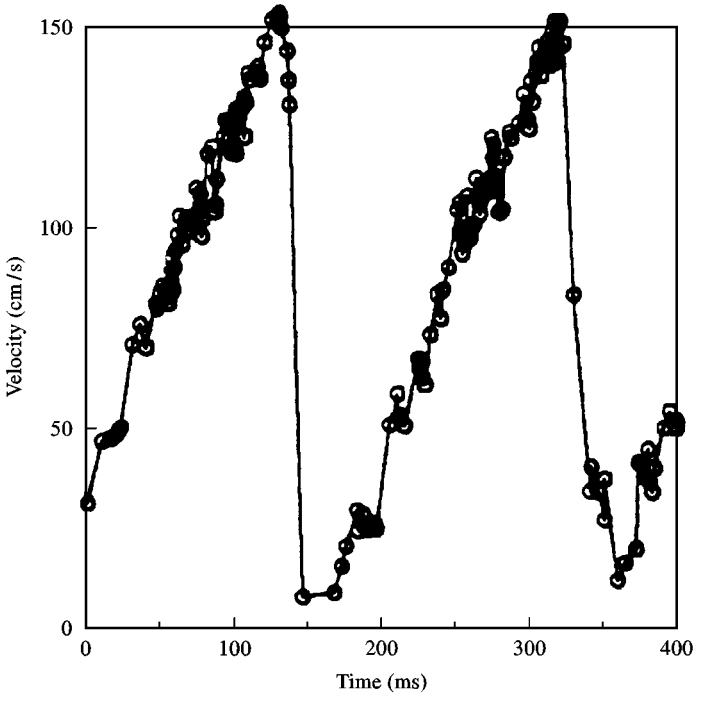

Figure 11. Time record of velocity ($x = 55$ mm).

two parameters due to the scattering of the data points. Four cases studied in the context of this work for which $P_e - \bar{P}_d$ increased are the following.

(a) Keeping Q constant and increasing P_e. Since $\bar{P}_d$ depends on the flow rate, this remains constant and therefore $P_e - \bar{P}_d$ increases.

(b) Keeping, P_e constant and (b_1) increasing the resistance of R_1 in this case the flow rate is reduced, and consequently $\bar{P}_d$ drops, so that $P_e - \bar{P}_d$ increases; (b_2) reducing the resistance of R_2; when the resistance of R_2 is reduced, $\bar{P}_d$ drops and therefore $P_e - \bar{P}_d$ increases; (b_3) increasing the elevation of the oscillating tube above the free surface of the lower level water tank; in this case, $\bar{P}_d$ is reduced and therefore $P_e - \bar{P}_d$ increases.

From the above four cases two characteristic examples could be mentioned. (i) Starting from a distended state, by increasing the resistance of R_1 and keeping $P_e = 200$ mm H_2O, the frequency increased from 0·6 to 1·6 Hz. The same trend but with higher frequencies was observed when repeating the experiment with higher P_e. (ii) In case that the elevation of the tube was changed from 150 to 350 mm and 650 mm above the lower water tank free surface, the frequency increased from 1·5 to 2·2 Hz and 5 Hz, respectively, with a mean flow rate of 800 ml/min and $P_e = 30$ mm H_2O.

It should be mentioned that although in the majority of the cases examined there was one distinct frequency of oscillation, in some cases there were one or two higher than this, of however, smaller energy content.

4. CONCLUSIONS

The flow field within a transparent self-excited flexible tube was examined through flow visualization, velocity and pressure measurements. The main observations made are as follows.

(a) The tube oscillations occurred under low and positive transmural pressures (of the order of 50 mm H_2O), independently of the external pressure, flow rate and settings of the constrictions. Under these pressures, the tube being compliant, was set to an oscillatory motion initiated by a flow asymmetry. According to this, the tube having the shape of a convergent–divergent nozzle, forced the flow to separate initially from both sides of its divergent section, but later on it became attached to one of them, being separated in the remaining part. When this flow asymmetry occurred, the opposite walls of the nozzle approached each other and the tube neck started oscillating streamwise, covering a distance of two diameters at the downstream edge of the tube. During the downstream motion of the neck, its area was progressively reduced, causing locally high velocities (twice) the inlet values, and a milder acceleration of the flow in the remaining part of the tube, for the additional reason that the total tube volume was reduced due to the shrinking process. When the neck approached the downstream edge of the tube, it expanded almost instantly causing a back flow in this area and a flow deceleration in the remaining part of the tube.

(b) The velocity amplitude increased streamwise, taking minimum values at its entrance and maximum values at its outlet. Downstream of the tube, the velocity increased almost linearly from a zero value to a maximum one, from which it dropped to zero almost instantly.

(c) There was a phase difference between the upstream and downstream of the tube pressure signals, the latter being in advance. That is, during the shrinking of the tube, the downstream pressure started first being reduced, whereas later on the upstream pressure started increasing, and specifically a little before the tube neck approached the end of the tube.

(d) The frequency of oscillations increased with increasing difference between the external pressure and the time-mean downstream pressure, without however being able to define a certain relationship between these two parameters.

ACKNOWLEDGEMENTS

Thanks are extended to Prof. N. Stergiopoulos of the Biomedical Engineering Laboratory of EPFL for allowing part of this work to be conducted in the facilities of this Lab, as well as to the valuable criticism of the reviewers.

References

Barclay, W. H. & Thalayasingam, S. 1986 Self-excited oscillations in thin walled collapsible tubes. *Medical and Biological Engineering and Computing* **24,** 482–487.

Bertram, C. D. 1986 Unsteady equilibrium behaviour in collapsible tubes. *Journal of Biomechanics* **19,** 61–69.

Bertram, C. D., Sheppeard, M. D. & Jensen, O. E. 1994 Prediction and measurement of the area–distance profile of collapsed tubes during self-excited oscillations. *Journal of Fluids and Structures* **8,** 637–660.

Bertram, C. D. & Godbole, S. A. 1995 Area and pressure profiles for collapsible-tube oscillations of three types. *Journal of Fluids and Structures* **9,** 257–277.

Brower, R. W. & Scholten, C. 1975 Experimental evidence on the mechanism for the instability of flow in collapsible vessels. *Medical and Biological Engineering* **XX,** 839–845.

Cancelli, C. & Pedley, T. J. 1985 A separated-flow model for collapsible tube oscillations. *Journal of Fluid Mechanis* **157,** 375–404.

Conrad, W. A. 1969 Pressure–flow relationships in collapsible tubes. *IEEE Transactions on Bio-Medical Engineering*, BME-**16,** 284–295.

Conrad, W. A., Cohen, M. L. & McQueen, D. M. 1978 Note on the oscillations of collapsible tubes. *Medical and Biological Engineering and Computing* **16,** 211–214.

Dion, B., Naili, S., Renaudeaux, J. P. & Ribreau, C. 1995 Buckling of elastic tubes: study of highly compliant device. *Medical and Biological Engineering and Computing*, **XX,** 196–201.

Elad, D. E., Sahar, M., Avidor, J. M. & Einav, S. 1992 Steady flow through collapsible tubes: measurements of flow and geometry. *ASME Journal of Biomechanical Engineering* **11,** 84–91.

Elliott, E. A. & Dawson, S. V. 1978 Fluid velocity greater than wavespeed and the transition from supercritical to subcritical flow in elastic tubes. *Medical and Biological Engineering and Computing* **17,** 192–198.

Griffiths, D. J. 1971 Steady fluid flow through veins and collapsible tubes. *Medical and Biological Engineering* **9,** 597–602.

Jensen, O. E. 1992 Chaotic oscillations in a single collapsible-tube model. *Journal of Biomechanical Engineering* **114,** 55–59.

Kamm, R. D. & Shapiro, A. H. 1979 Unsteady flow in a collapsible tube subjected to external pressure or body forces. *Journal of Fluid Mechanics* **95,** 1–78.

Matsuzaki, Y., Ikeda, T., Kitagawa, T. & Sakata, S. 1994 Analysis of flow in a two-dimensional collapsible channel using universal "tube" law. *Journal of Biomechanical Engineering* **116,** 469–476.

Morgan, P. & Parker, K. H. 1989 A mathematical model of flow through a collapsible tube I., model and steady flow results. *Journal of Biomechanics* **22,** 1263–1270.

Pedley, T. J. 1992 Longitudinal tension variation in collapsible channels: a new mechanism for the breakdown of steady flow. *Journal of Biomechanical Engineering* **114,** 60–67.

Pythoud, F., Stergiopoulos, N. & Meister, J.-J. 1994 Modeling of the wave transmission properties of large arteries using nonlinear elastic tubes. *Journal of Biomechanics* **27,** 1379–1381.

Ribreau, C., Naili, S., Bonis, M. & Langlet, A. 1993 Collapse of thin-walled elliptical tubes for high values of major to minor axis ratio. *Journal of Biomechanical Engineering* **115,** 432–440.

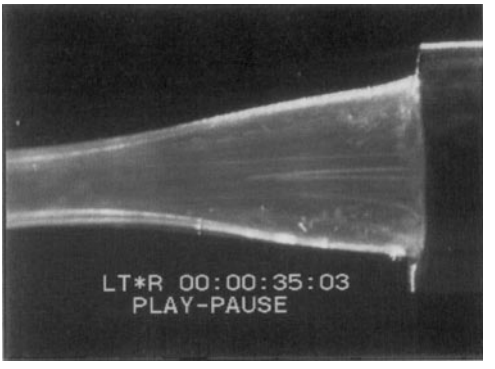

Figure 1. Symmetric flow-field about jet axis.

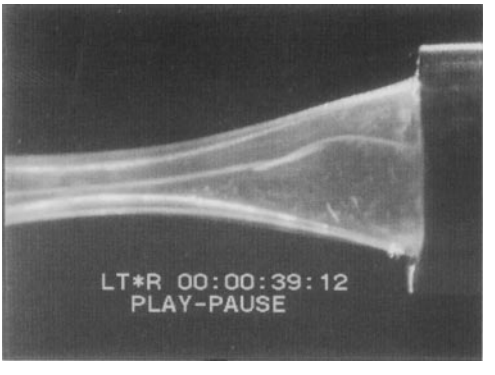

Figure 2. Flow attached to one side of the tube-divergent nozzle.

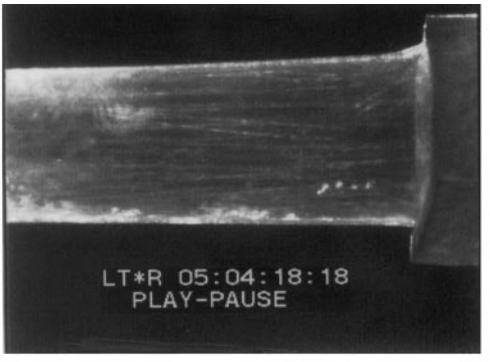

Picture 1

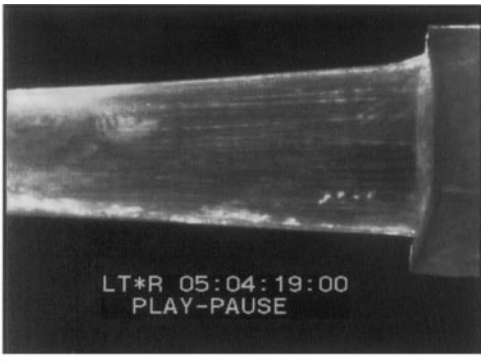

Picture 2

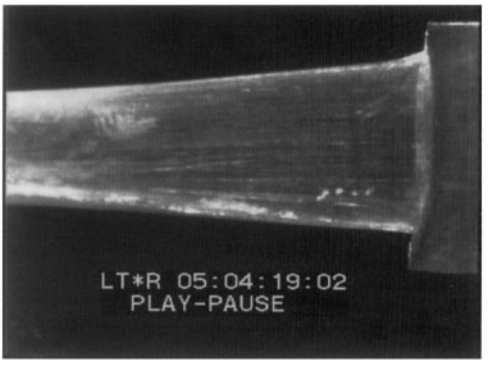

Picture 3

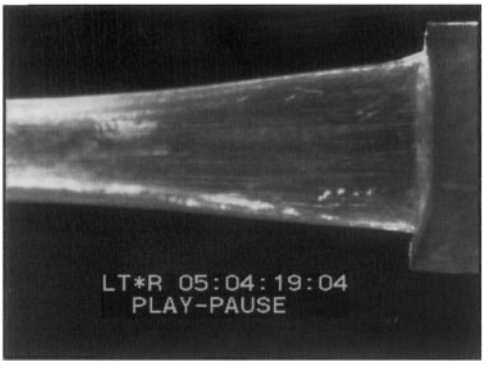

Picture 4

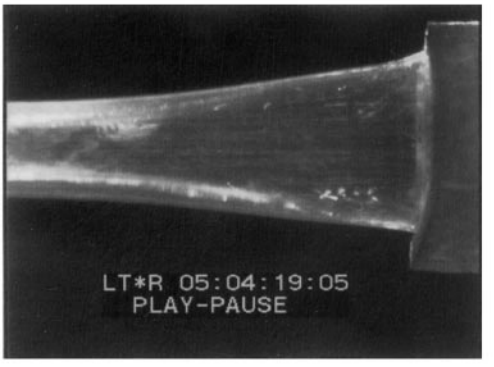

Picture 5

(a)

Figure 3. (a) Pictures of the oscillating tube. Flow from left to right. (b) Picture of the oscillating tube (cont.)

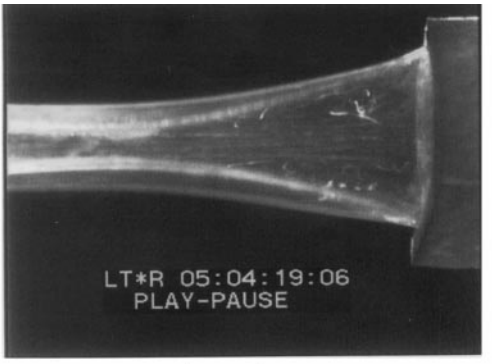

Picture 6

Picture 7

Picture 8

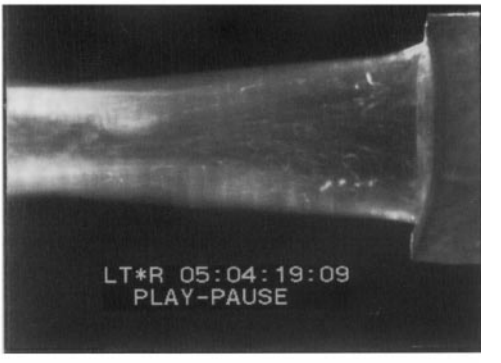

Picture 9

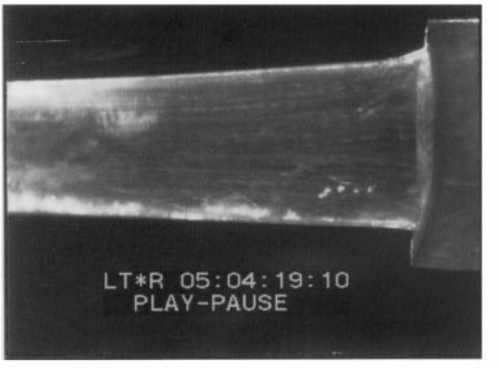

Picture 10

(b)

Figure 3. (Continued).